2023 IEEE/ASME International Conference on Advanced Intelligent Mechatronics (AIM)
June 28-30, 2023. Seattle, Washington, USA

Improving Human Positioning Control of Oscillatory Systems

Man Wo Lui*[1], Daniel Kotten*[1], Enea Dushaj*[1], William Singhose[1]

***Abstract*— Flexible systems are difficult to control because they deflect in response to any applied force and they tend to oscillate around the desired path or set point. Human operators driving such systems are challenged by the deflection and vibration that makes the system difficult to move and accurately position. Such systems can be augmented with an intelligent control scheme that aids the human operator. Numerous types of controllers can be used for such applications; however, it is challenging to balance the control authority of the human operator and the augmenting controller. Input shaping is a control technique that reduces unwanted flexible system responses by modifying the human-operator command in real-time. This paper investigates the use of input shaping as an augmenting controller to aid in the accurate positioning of highly-oscillatory systems. Results from operator testing verify some of the key advantages of this controller.**

I. Introduction

Flexible systems are difficult to control because they respond to human-operator commands with deflection and residual vibrations that make it challenging to move and accurately position the system. Input shaping is a control technique that reduces unwanted flexible responses by modifying the human-operator command in real-time. This modification is accomplished by convolving the operator input with a series of impulses, to attenuate unwanted vibration responses.

The penalty introduced by input shaping is a lengthening of the shaped command by an amount equivalent to the duration of the input shaper (typically 0.5-1.5 vibration periods). This increase in command duration not only increases the rise time of the shaped command, but can cause some system motion, or overtravel, after the human operator has commanded the system to stop. This additional motion contributes to suppressing the vibration excited during the deceleration portion of the command. However, to accurately position a system, the human operator must estimate this overtravel. This effect may make precise positioning of the system difficult. Using longer-duration shapers, such as those designed to be extremely robust to parameter variations or to eliminate multiple modes of vibration, can exacerbate this effect.

Input-shaped step sequences may consist of many step commands. The amplitudes and execution times of the steps in a shaped command may be represented in matrix form as:

$$\begin{bmatrix} A_i \\ t_i \end{bmatrix} = \begin{bmatrix} A_1 & \dots & A_i & \dots & A_N \\ t_1 & \dots & t_i & \dots & t_N \end{bmatrix} \quad (1)$$

where A_i are the step amplitudes as a proportion of maximum actuator effort, t_i are the times of step execution, and N is the number of impulses. Input shapers can be designed with robustness to errors and changes in system parameters [1], [2]. The profile of an unshaped velocity command is compared to that of an input-shaped command in Figure 1 [3]. The stop command is issued at the beginning of the shaded areas. These areas represent the distance the system travels after the stop command has been issued.

[1]Woodruff School of Mechanical Engineering, Georgia Institute of Technology, Atlanta, GA, USA. Contact: singhose@gatech.edu.
*These authors contributed equally to this work.

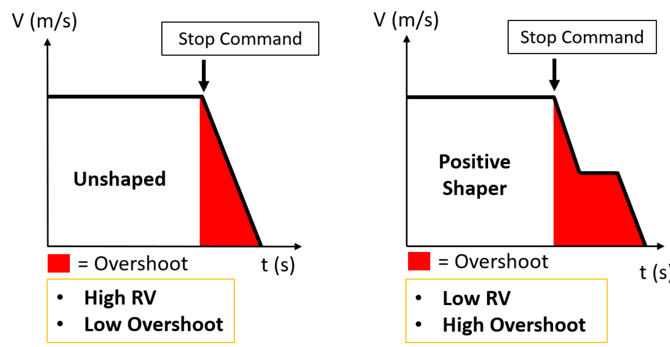

Fig. 1. Position overshoot for unshaped and positive shapers.

The shaper duration, position overshoot, and robustness for various input shapers are tabulated in Table I [4]. The "Shaper Robustness" column is the normalized range of frequencies that the associated shaper attenuates to below 5% of the unshaped residual vibration. The normalization is done with respect to the ZV shaper frequency range, centered about the design frequency of the shaper. It can be observed that the more robust a shaper is, the longer the shaper duration, and thus the larger the final position overshoot. This is especially of concern when operating a crane in a crowded environment, as well as in other scenarios requiring precise positioning. Therefore, the operator must compensate for this overtravel, as well as the overtravel occurring from the inherent deceleration, as shown on the left plot of Figure 1. While the reduction in overshoot from input shaping has been studied in space and robotics applications [5] [6], the overshoot in crane systems due to input shaping is the focus of this work.

Feedback controllers are challenging to implement on cranes because the payload motions can be difficult to accurately and reliably sense [7]. It is also important to note that virtually all cranes are human-operated. Therefore, swing-control algorithms must integrate well with human operators. Control systems that induce unexpected movements can annoy crane operators and induce safety concerns. Additionally, the crane operator should be treated as a nonlinear time-varying feedback control system that must take precedence over the auxiliary swing controller.

Rather than relying on feedback control, payload swing can be reduced by filtering the operator commands [1], [4],

TABLE I

SHAPER DURATION, POSITION OVERSHOOT, AND ROBUSTNESS.

		Metrics		
		Final Position Overshoot [mm]	Shaper Duration [s]	Shaper Robustness Range Relative to ZV Robustness Range [ω_r/ω_{r_ZV}]
Standard Shaper	NEG ZV	35	0.79	0.8
	NGUMZV	46	0.91	0.8
	ZV	68	1.36	1.0
	NEG ZVD	92	1.85	3.8
	NEG EI	92	1.87	5.3
	ZVD	137	2.73	4.4
	EI	137	2.73	6.2
New Shapers	ZV - PP	0	2.05	0.5
	NEG ZV - PP	0	1.82	0.5

[8]. Using this approach, the human operator is the only feedback control system. These types of operator-shaping methods integrate well with humans, as verified by several operator performance studies [9]–[11]. Given its simple structure and effective results, human-command shaping has been implemented on hundreds of cranes [9], [10], [12]–[16].

The philosophy for the development of the control scheme presented in this paper was influenced by the techniques discussed in US Patent 8,975,853 [11]. This patent describes the development of a "Reduced Overtravel" (RO) input shaper, that aims to use an input-shaping control method to minimize overshoot in a physical system. The RO has an additional constraint characterized by:

$$\bar{x}^{+} \equiv \frac{1}{\tau}\sum_{i=1}^{n} A_i t_i \le \bar{x}^{+}_{des} \tag{2}$$

τ is the period the shaper is designed to attenuate, A_i and t_i are the amplitude of the impulse and its respective execution time, and $\bar{x}$ and $\bar{x}_{des}$ are the overtravel and the desired amount of shaper-induced overtravel respectively.

Multiple methods for constructing precise positioning (PP) shapers exist. Optimization of the constraint equations can yield short precise positioning shapers, however, these shapers tend to have poor robustness. This paper describes a method for converting any shaper into a PP shaper. This is done by convolving a seed shaper, the shaper of interest, with itself and an inverse of itself, separated by short time intervals. This paper also explores the effectiveness of precise position shapers on human subjects by comparing the performance of bridge crane operators performing a pickup and delivery task. Three different cases were tested – a traditional shaper with overtravel, a PP shaper, and no shaping. The effectiveness of each shaper for users of varying experience levels was evaluated by recording the success of each user and their position error of payload placement during testing. This gives insight into the intuitiveness of traditional shapers versus the precise positioning shapers developed in this paper, as well as the effectiveness of various shapers in reducing system vibration and improving the positioning precision [17].

II. REQUIREMENTS OF INPUT SHAPERS

Input shapers may be designed using different combinations of performance requirements. For example, one set of constraints consists of requiring zero residual vibration at the time of the last impulse and restricting the impulses to be positive. The residual vibration resulting from a sequence of impulses applied to an underdamped system can be calculated using:

$$V(\omega,\zeta) = e^{-\zeta\omega t_n}\sqrt{[C(\omega,\zeta)]^2 + [S(\omega,\zeta)]^2} \tag{3}$$

where

$$C(\omega,\zeta) = \sum_{i=1}^{n} A_i e^{\zeta\omega t_i} cos(\omega_d t_i) \tag{4}$$

$$S(\omega,\zeta) = \sum_{i=1}^{n} A_i e^{\zeta\omega t_i} sin(\omega_d t_i) \tag{5}$$

The symbols ω and ζ are the target frequency to be suppressed, and the damping ratio of the flexible mode, respectively. The symbol n represents the number of impulses in the impulse sequence, t_n is the time location of the final impulse, and the damped natural frequency is characterized as:

$$\omega_d = \omega\sqrt{1-\zeta^2} \tag{6}$$

When V is set to zero, (3) results in a zero residual vibration constraint. Due to the transcendental nature of (3), there are multiple solutions that yield zero residual vibration. To make the solution time optimal and subject to the zero residual vibration and amplitude constraints, the input shaper duration must be as short as possible. For an undamped flexible mode, a ZV input-shaper [4] has amplitudes and times of:

$$\begin{bmatrix} A_i \\ t_i \end{bmatrix} = \begin{bmatrix} 0.5 & 0.5 \\ 0 & \frac{1}{2}T_n \end{bmatrix} \tag{7}$$

where T_n is the target oscillation period to attenuate.

In order for the system to return to the position where the stop command was given, the area under the velocity versus time profile after the stop command until the trolley stops moving must be equal to zero. This is represented by the integral:

$$\int_{t_{stop}}^{t_{final}} v\,dt = 0 \tag{8}$$

To ensure that the crane trolley will not be over-actuated, the running sum of amplitudes can be limited to less than 2:

$$\left|\sum_{i=1}^{j} A_i\right| \le 2,\; j \in (1,n) \tag{9}$$

III. PRECISE POSITIONING SHAPERS

The basic idea of constructing the precise positioning shaper is demonstrated using ZV shapers [1]:

$$\text{ZV Shaper:} \begin{bmatrix} A_i \\ t_i \end{bmatrix} = \begin{bmatrix} -0.5 & -0.5 \\ 0 & \frac{1}{2}T_n \end{bmatrix} \tag{10}$$

Three ZV shapers (10) are used: the initial deceleration shaper, the acceleration of the move-back shaper, and the deceleration of the move-back shaper. The deceleration and acceleration portion of the move-back shaper is combined to form the full move-back shaper, which moves the trolley back to the desired stop position. By starting the deceleration portion of the move-back shaper ¼ of the target period after the initial

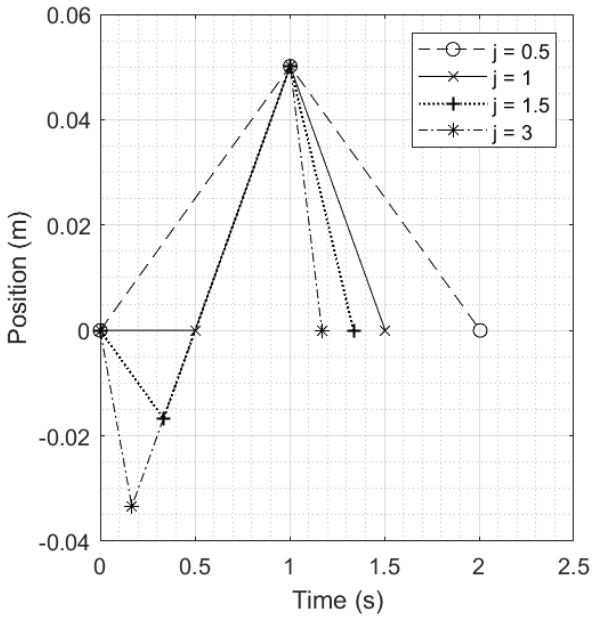

Fig. 2. Effect of Go Back Multiplier "j".

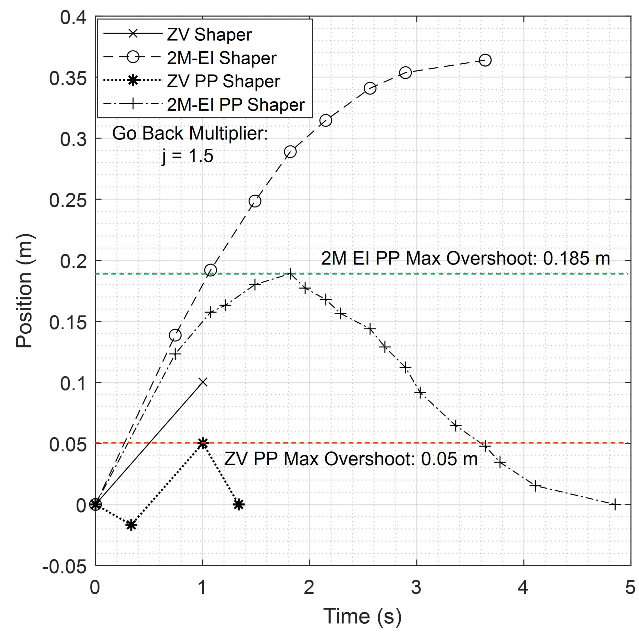

Fig. 3. Comparison of Overshoot and Settling Time.

deceleration impulse for a ZV shaper, the trolley will be able to move back to the desired position:

$$\begin{bmatrix} A_i \\ t_i \end{bmatrix} = \begin{bmatrix} -0.5 & 0.5 & -0.5 & 0.5 \\ 0 & \frac{1}{4}T_n & \frac{1}{2}T_n & \frac{3}{4}T_n \end{bmatrix} \quad (11)$$

The deceleration shaper and the move-back shaper (11) are combined to form the ZV Perfect Positioning Shaper:

$$\begin{bmatrix} A_i \\ t_i \end{bmatrix} = \begin{bmatrix} -1 & 0.5 & -1 & 0.5 \\ 0 & \frac{1}{4}T_n & \frac{1}{2}T_n & \frac{3}{4}T_n \end{bmatrix} \quad (12)$$

A generalized equation for the construction of the PP shaper can be obtained. The original deceleration shaper is combined with the acceleration shaper of the move-back command. The deceleration shaper of the move back command is then inserted starting from k seconds $(0 < k \le t_n)$ after the initial step impulse at 0 seconds. Furthermore, the move-back portion can be scaled by a factor j, $(0 < j \le 2)$, which represents the "go back multiplier":

$$\begin{bmatrix} A_i \\ t_i \end{bmatrix} = \begin{bmatrix} -(1+j)A_0 & jA_0 & -(1+j)A_1 & jA_1 & \cdots \\ 0 & k & t_1 & k+t_1 & \cdots \end{bmatrix}$$
$$\begin{matrix} -(1+j)A_{n-1} & jA_{n-1} & -(1+j)A_n & jA_n \\ t_{n-1} & t_{n-1}+k & t_n & t_n+k \end{matrix}\Bigg] \quad (13)$$

The larger the multiplier j, the quicker the precise positioning shaper will return the trolley back to its desired location, but at the cost of decreased robustness. The effect of j on the settling time for a ZV shaper is shown in Figure 2. When $j = 0.5$, it takes 2 seconds for the ZV PP shaper to arrive at the desired position ($0m$). As j increases, the time it takes for the trolley to arrive at the desired position decreases. The duration decreases to 1.5 seconds for $j = 1$, and to 1.17 seconds for $j = 3$. It must be noted that larger go-back multipliers require larger negative impulses, which will excite high-mode frequencies.

To generate the precise positioning shaper, the value of k that results in the shaper in (13) that satisfies (2) must be determined. This method of generating PP shapers can be applied to any positive shaper. The value of k can be solved numerically. For example, the built-in MATLAB function $fzero()$ can be used to determine the value k that satisfies (2). The function can also account for the overshoot distance due to the deceleration of an unshaped command:

$$\text{Overshoot Distance} = \frac{1}{2}\frac{v_{max}^2}{a_{max}} \quad (14)$$

This zero-total overshoot can be achieved by increasing k to travel back further and compensate for the total overshoot distance. However, a PP shaper that meets this constraint results in a longer duration shaper compared to the original shaper. This also results in an overshoot of the desired position. The comparison of the overshoot and the settling time between a ZV and two-mode (2M) EI shaper with their precise positioning counterparts (with $j = 1.5$) are shown in Figure 3. Comparing the ZV shaper and the precise positioning shaper created from it, the maximum overshoot of the ZV shaper is $0.1m$. Although the PP shaper stops at a final position of $0m$, it has a maximum overshoot of $0.05m$. This is due to the sequence of impulses for a shaper not occurring instantaneously. The PP shaper reaches its maximum overshoot at the same time as the ending time of the original ZV shaper, and its settling time is 1.34 seconds. Just as a 2M EI shaper has a longer duration than a ZV shaper, a 2M EI precise positioning (2M EI-PP) shaper has a longer duration than a ZV PP shaper. The 2M EI-PP shaper presented in Figure 3 has a settling time of 4.85 seconds and a maximum overshoot of $0.185m$, compared to a settling time of 3.64 seconds and a maximum overshoot of $0.31m$ corresponding to the original 2M EI shaper.

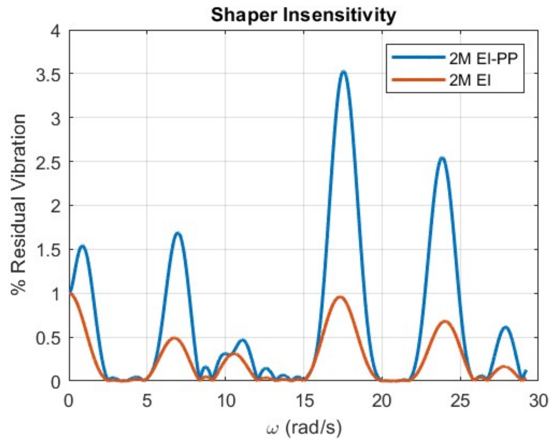

Fig. 4. 2-Mode EI and Precise Positioning 2-Mode EI Shaper Insensitivity.

Additionally, precise positioning shapers can be implemented by solving an optimization problem with the constraints described above. Precision positioning shapers obtained via optimization can yield shapers that are nearly the same duration as the original shaper. As a trade-off, optimized precise positioning shapers tend to be less robust than precise positioning shapers constructed using the generic method described above. Furthermore, multi-mode PP shapers and robustness constraints may be implemented via optimization. However, this extension is not covered in this paper.

A. 2-Mode EI Precise Positioning Shaper

A 2M EI-PP shaper was generated for a small-scale crane by solving (2) and (13) using MATLAB. This allows for near-zero position deviation from the stop command to be achieved while maintaining zero residual vibration. The 2M EI-PP shaper parameters are:

$$\begin{bmatrix} A_i \\ t_i \end{bmatrix} = \begin{bmatrix} -0.17 & -0.31 & -0.31 & 0.10 & -0.17 & -0.57 & \cdots \\ 0 & 744 & 1075 & 1213 & 1489 & 1819 & \cdots \end{bmatrix}$$
$$\begin{matrix} 0.19 & -0.17 & 0.19 & -0.31 & 0.10 & -0.31 & \cdots \\ 1957 & 2150 & 2288 & 2564 & 2702 & 2894 & \cdots \end{matrix}$$
$$\begin{matrix} 0.33 & 0.10 & -0.17 & 0.19 & 0.19 & 0.10 \\ 3033 & 3364 & 3769 & 3777 & 4108 & 4853 \end{matrix} \quad (15)$$

where t_i is in milliseconds. This was designed to cancel frequencies around $2.9 rad/s$ and $4.2 rad/s$, the natural frequencies of the double-pendulum bridge crane hook and payload system.

The robustness of this shaper is characterized by the insensitivity plot shown in Figure 4. At the higher design frequency, the PP version is more sensitive to errors, as expected for a shaper that uses negative impulses. With high-mode excitation errors, the PP shaper is likely to have a higher percent residual vibration than other shaper designs. The precise positioning shaper limits positional deviation and minimizes residual vibration. This is at the cost of an increased command duration, increased actuator effort, and decreased robustness.

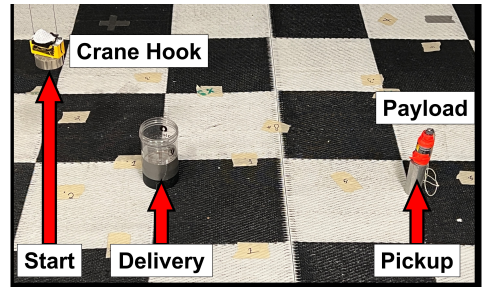

Fig. 5. Crane Starting Position.

Fig. 6. Payload Delivery.

IV. Human Operator Testing of 2-Mode EI Precise Positioning Shaper

Human operator tests were conducted on a small-scale bridge crane to determine the robustness of precise positioning shapers and to evaluate the effect of input shapers on the ability of human operators to control a flexible system accurately. Tests were performed with 16 operators to determine the efficacy and intuitiveness of the PP shaper. Users were tasked with picking up a payload and delivering it to a target location.

A. Protocol for Human Operator Verification Tests

The human operator tests were conducted in a Georgia Tech Lab using a crane driven by a Siemens PLC. The crane trolley was set to move at a maximum speed of $0.2 m/s$. At the start position shown in Figure 5, the magnetic hook of the crane was suspended at a length of approximately $1700 mm$ from the trolley. Operators were first tasked with moving the crane to pick up the payload located at a horizontal distance of $900 mm$ from the starting position. Operators were then tasked with lowering the crane hook to pick up the payload. The payload was attached to the crane hook via magnets. Then they were tasked with hoisting the payload up and suspending it approximately $1700 mm$ from the crane trolley. Finally, operators were tasked to deliver the payload to a target located $500 mm$ from the pickup location, as shown in Figure 6.

Operators were allowed one move event to adjust the location of the trolley, and as many movements in the Z (Hoist) direction as needed. Each user performed the test: 1) with no shaping, 2) with 2M ZV acceleration shaping & 2M EI deceleration shaping, and 3) with 2M ZV acceleration shaping & 2M EI-PP deceleration shaping. The 2M EI-PP shaper allowed for vibration control of the single-pendulum system before payload pickup, as well as the double-pendulum system after pickup. A two-mode shaper was also chosen for this testing as it would be effective at reducing vibration when the crane was and was not carrying the payload. When

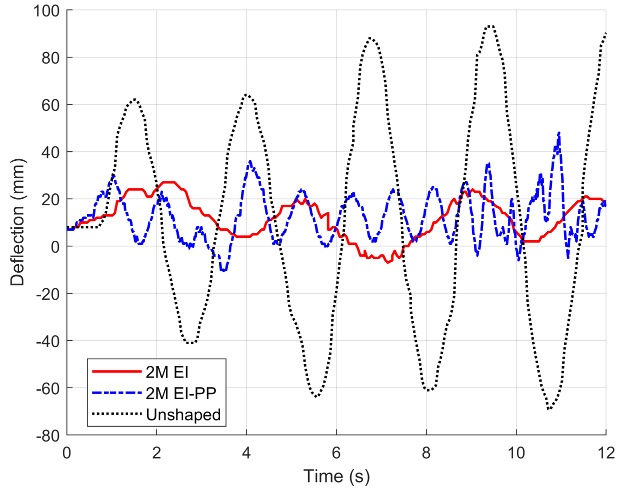

Fig. 7. Payload Deflection of Different Shapers for Human Tests.

running the experiments, some test subjects were selected to perform the test with each shaper without being told how the shaper would impact the movement of the trolley. They then performed the test again with the two input-shaping methods, with the expected movement caused by the shaper explained to the test subject.

After each move, the final trolley position was recorded, and the error from the desired position was calculated. The self-reported crane operation experience level of each user was recorded as beginner, intermediate, or advanced. In general, beginner users had minimal experience with a crane before, intermediate users had experience with cranes without input shaping or minimal experience with cranes that utilize input shaping, and advanced users had a great deal of experience with cranes with and without input shaping. Across the 16 test subjects, 6 described their crane operation experience as beginner, 4 as intermediate, and 6 as advanced.

B. Human Operator Test Results

The effectiveness of input shapers at reducing steady-state payload deflection is demonstrated by the results collected from the human operator trials. An example set of time responses is shown in Figure 7. It can be concluded that the 2M EI and the 2M EI-PP input shapers successfully reduced the payload deflection. The ability of the precise positioning shaper to increase the control accuracy of a human operator will be further analyzed and discussed.

Box and whisker plots of position error for each shaper and for each experience level for all *pickup* trials are shown in Figure 8. The pickup phase was the first phase performed by each user. Similar plots of position error for each shaper and for each experience level for all *delivery* trials are shown in Figure 9. In the delivery phase, all test subjects performed better while using the input shapers, getting closer to the desired position on average, with the spread of error decreasing. Test subjects tended to overshoot the desired position with the 2M EI shaper, but they slightly undershoot with no shaper and with the 2M EI-PP shaper. On average, the PP shaper resulted in the lowest errors.

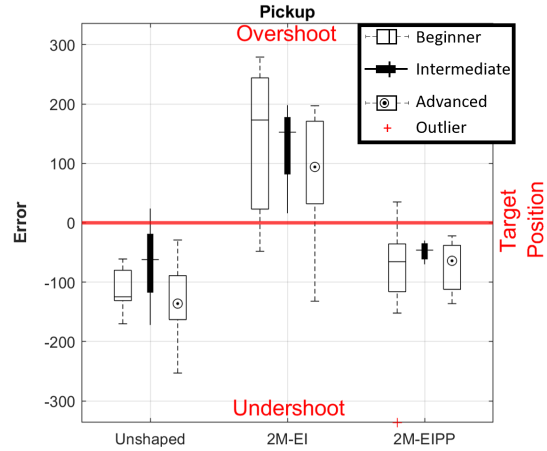

Fig. 8. Box and whisker plots of positioning error for all pickup trials.

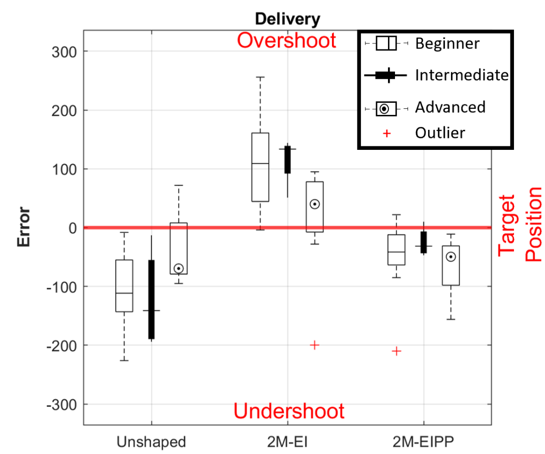

Fig. 9. Box and whisker plots of positioning error for all delivery trials.

TABLE II
ABSOLUTE MEAN DIFFERENCE OF DISTANCE ERROR.

Shaper	Mean Difference of Distance Error (mm)		
	Unshaped & 2M EI	2M EI & 2M EI-PP	Unshaped & 2M EI-PP
Pickup	229.90	193.50	36.40
Delivery	164.48	128.75	35.73

To determine if the difference in human operator performance and control accuracy was due to the effect of the input shaper or random probability, ANOVA tests were conducted on the pickup and delivery trial data. The pickup and delivery error data between the unshaped, 2M EI and 2M EI-PP had ANOVA Test result p-values of 2.47×10^{-12} and 2.82×10^{-9} respectively. This shows that the probability of the trend between the different shapers being due to random chance is extremely low. Therefore, it can be concluded that precise positioning shapers have a significant effect on the increase of human operator control accuracy. Performing posthoc tests on the ANOVA test results, the absolute mean difference between Unshaped and 2M EI, Unshaped and 2M EI-PP, and 2M EI and 2M EI-PP for the pickup and delivery trials is shown in Table II. It can be concluded that 2M-EIPP shaper greatly increases the intuitiveness of the control, allowing human operators to achieve significantly higher precision.

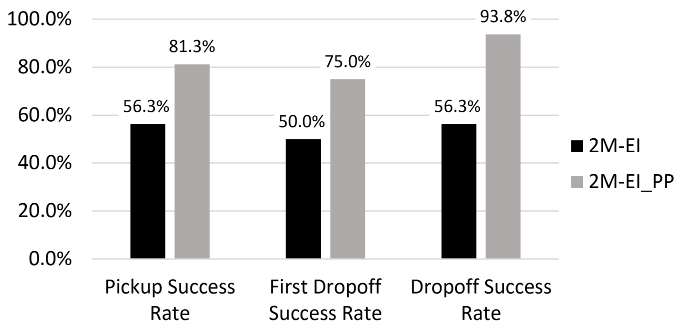

Fig. 10. Traditional Shaper vs PP Shaper Task Success Rate.

The difference in the effectiveness of the input shapers based on the experience level of the operator is also evident in Figure 8 and Figure 9. It can be observed that the 2M EI-PP shaper equalizes the accuracy of operator performance across the different experience levels. The 2M EI-PP shaper allowed beginner-level test subjects to achieve accuracy levels comparable to those of experienced test subjects.

The success rates of each task for the two input-shaped trials of each user are shown in Figure 10. Both pickup and delivery success rates increased with the tested PP shaper. First-try pickup and delivery success rates (only one move in the Z-direction) were both 25% greater with the 2M EI-PP Shaper than the regular 2M EI Shaper. Considering trials where users tried multiple movements in the Z-direction, pickup, and delivery success rates were 37.5% higher with the 2M EI-PP Shaper than the regular 2M EI shaper. These results demonstrate the effectiveness of the PP shaper for completing the tasks described and are a testament to the ease of use of the shaper.

C. Operator Feedback

In general, novice test subjects preferred the PP Shaper. They described it as intuitive because the control scheme caused the system to operate as expected based on their limited experience with other machines. Some novice test subjects preferred no input shaping on their controls, as the crane could respond faster to their input. However, the consequent high vibration amplitudes were reported as difficult to compensate for among these test subjects.

Experienced test subjects showed no preference between the two shaped inputs, as long as they had time to train on the specific shaper. A theme in the experienced user feedback was that the PP shaper control scheme was, "easy to use," and "performed consistent with their experience." However, the long shaper duration made the crane difficult to control using a fast series of inputs. In their feedback, the attenuation of the higher vibration mode was particularly helpful. Two test subjects preferred the 2M EI shaper with $350mm$ of overshoot. They felt it was easier to predict overshoot than to time the alignment of the hook/payload with their desired position. In general, however, many test subjects expressed satisfaction with the PP shaper, and results indicated improved positioning error and higher trial success rates. The PP shaper is naturally intuitive as well, as test subjects, in general, expect some small overshoot, but not the large amount of overshoot that can occur with the 2M EI shaper.

V. Conclusions

This paper investigated the ability of human operators to precisely position oscillatory systems. Traditional input shapers were found to lead to overshoot of the desired position. A new form of input shaper was developed to allow test subjects to arrive at a final position more accurately. Human testing using 16 operators verified the utility of the new input-shaping algorithm. Furthermore, this technology is able to assist users across all crane operator skill levels.

References

[1] N. C. Singer and W. P. Seering, "Preshaping command inputs to reduce system vibration," *Journal of Dynamic Systems, Measurement, and Control*, vol. 112, pp. 76–82, March 1990.

[2] W. Singhose, W. Seering, and N. Singer, "Input shaping for vibration reduction with specified insensitivity to modeling errors," in *Japan-USA Sym. on Flexible Automation*, vol. 1, Boston, MA, 1996, pp. 307–13.

[3] R. Z. Pu Zhao, Yunfei Zhou, "A new trajectory optimizing method using input shaping principles," *Shock and Vibration*, vol. 2018, 2018.

[4] O. Smith, *Feedback Control Systems*. New York: McGraw-Hill Book Co., Inc., 1958.

[5] P. H. SiRupert, Levi and M. D. Killpack, "Comparing model predictive control and input shaping for improved response of low-impedance robots," *2015 IEEE-RAS 15th International Conference on Humanoid Robots (Humanoids)*, vol. 2015, p. 256–263, 2015.

[6] W. C. T. T. Zhao, Yu and M. Tomizuka, "Zero time delay input shaping for smooth settling of industrial robots," *2016 IEEE International Conference on Automation Science and Engineering (CASE)*, vol. 2016, p. 620–625, 2016.

[7] Y. Jung, I. G. Jang, B. M. Kwak, Y.-K. Kim, Y. Kim, S. Kim, and E. H. Kim, "Advanced sensing system of crane spreader motion (for mobile harbor)," in *IEEE International Systems Conference*, 2012, pp. 59–63.

[8] T. Vyhlidal and M. Hromik, "Parameterization of input shapers with delays of various distribution," *Automatica*, vol. 59, pp. 256–263, 2015.

[9] D. Kim and W. Singhose, "Performance studies of human operators driving double-pendulum bridge cranes," *Control Engineering Practice*, vol. 18, no. 6, pp. pp. 567 – 576, 2010.

[10] A. Khalid, J. Huey, W. Singhose, J. Lawrence, and D. Frakes, "Human operator performance testing using an input-shaped bridge crane," *Journal of Dynamic Systems, Measurement and Control*, vol. 128, no. 4, pp. pp. 835 – 841, 2006.

[11] J. Vaughan, P. Jurek, and W. Singhose, "Reducing overshoot in human-operated flexible systems," *Journal of Dynamic Systems, Measurement, and Control*, vol. 133, no. 1, p. 011010, 2011.

[12] K.-T. Hong and K.-S. Hong, "Input shaping and vsc of container cranes," in *IEEE International Conference on Control Applications*, Taipei, Taiwan, 2004, Conference Proceedings, pp. 1570–1575.

[13] K. Sorensen, W. Singhose, and S. Dickerson, "A controller enabling precise positioning and sway reduction in bridge and gantry cranes," *Control Engineering Practice*, vol. 15, no. 7, pp. 825–837, 2007.

[14] S.-W. Hong, G.-H. Bae, and B.-G. Kim, "Development of miniature tower crane and payload position tracking system using web-cam for education," in *IASTED Int. Conference on Robotics and Applications*, Cambridge, MA, 2010.

[15] J. Vaughan, A. Karajgikar, and W. Singhose, "A study of crane operator performance comparing pd-control and input shaping," in *American Control Conference (ACC), 2011*, 29 2011-july 1 2011, pp. 545 –550.

[16] Z. N. Masoud and K. A. Alhazza, "Frequency-modulation input shaping control of double-pendulum overhead cranes," *ASME J. Dynamic Systems, Measurement and Control*, vol. 136, no. 2, 2014.

[17] W. Vaughan J., Singhose, "Input shapers for reducing overshoot in human-operated flexible systems," *American Control Conference*, vol. 5160187, pp. 178–183, June 2009.